

Synthesis and Characterization of Crystalline Nano TiO₂ and ZnO and their Effects on the Photodegradation of Indigo Carmine Dye

Badr A. El-sayed, Ibrahim A. Ibrahim, Walied A. A. Mohamed, Mahmoud A. M. Ahmed

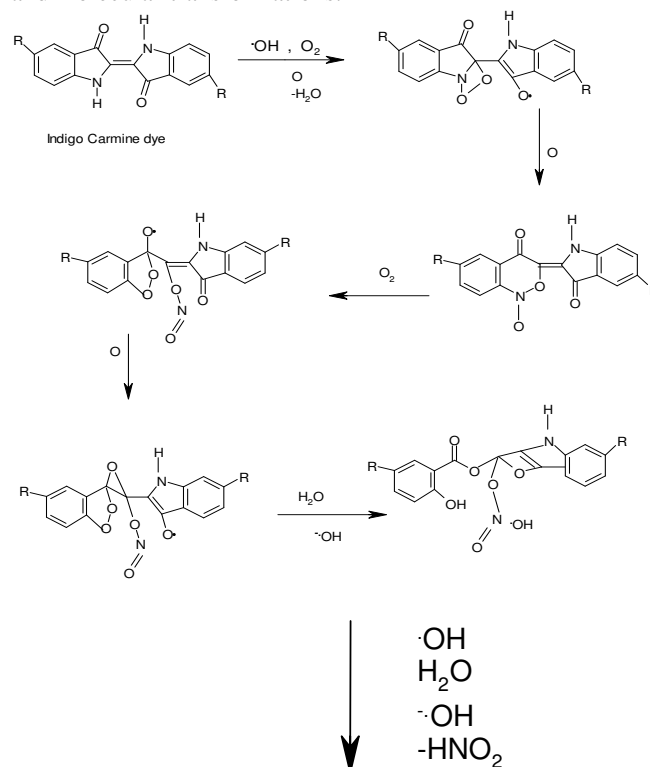
Abstract - TiO₂ and ZnO as nanoparticles have been synthesized and characterized using powder X-Ray Diffraction (XRD) and Scanning Electron Microscope (SEM). The study of photocatalytic Activity using the synthesized TiO₂ and ZnO in commercial and nano forms on the photodegradation of indigo carmine dye under UV irradiation has been carried out. The photodegradation was monitored by measuring the change of dye concentration as a function of irradiation time with power of UV lambs (254, 312 and 354 nm). The optimum of indigo carmine concentration was initially determined; the effects of different pH's on the photodegradation of IC have been studied in the range of (3 - 13.5) under UV irradiation. Also pK_a of the dye was determined by two methods. The photocatalytic effects of different amounts of the synthesized nano particles of TiO₂ (28 nm) and ZnO (34 nm) on the photodegradation rates were of the first-order reaction, and mechanism of photodegradation of the dye was discussed. It is observed that the rate of photodegradation process increasing with the nano particles of the synthesized oxides TiO₂ (28 nm) and ZnO (34 nm) comparable to their commercial oxides.

Keywords: Indigo carmine (IC), nano oxides, pK_a and photocatalytic degradation.

I. INTRODUCTION

Synthetic dyes are used almost in all branches of the consumer goods industry. About 10 000 tons of dyes are produced per year¹. Inevitably, there are losses (approximately 12 % of used amount) during manufacturing and processing operations. The effluents dyes is resistant to the light or other degradative environmental conditions, it is necessary to remediate these effluents before they are released to the environment. However, common wastewater treatment plants are ineffective in removal of dyes from the wastewaters. One of possible options to modify these facilities to get better outcome is an application of the Advanced Oxidation Processes (AOPs), i.e., chemical methods based on generation of highly reactive hydroxyl radicals. Semiconductors such as ZnO and TiO₂ are often used as photocatalytic agents because of their high stability, low costs, high efficiency and nil toxicity. They are gaining much importance for their using with issues like environmental pollution and energy generation²⁻⁴. In the present study we have synthesized TiO₂ (28 nm) and ZnO (34 nm) which exhibit higher photocatalytic activity under the UV light irradiation⁵.

The AOPs includes heterogeneous photocatalysis capable of a degradation of a wide range of organic compounds including the dyes⁶⁻⁷. Photocatalytic activity of TiO₂ can be substantially affected by its crystalline structure. A Probable reaction mechanism of the photocatalytic degradation of indigo carmine dye in presence of TiO₂: AlPO₄-5 Zeolites can be described according to the following steps⁸ (**Scheme 1**). The technology of heterogeneous photocatalysis is based on the irradiation of a semiconduction photocatalyst. Semiconductors are characterized by a narrow band gap between their valence and conduction bands (VB and CB respectively). The absorption of a quantity of luminous energy being greater than or the same as the band gap (E_g) of the semiconductor results in an abrupt transfer of electrons from valence to the conduction and the consequent creation of holes (h⁺) in of indigo carmine dye the valence band. Such charge transfer introduces some unbalanced conditions, which lead to the reduction or oxidation of the species adsorbed onto the surface of the semiconductor⁹. A heterogeneous photocatalytic system consists of semiconductor particles (photocatalyst), which are in close contact with a liquid or gaseous reaction medium. Exposing the catalyst to light excited states is generated, which are able to initiate subsequent Processes like redox reactions and molecular transformations.



Revised Version Manuscript Received on November 15, 2015.

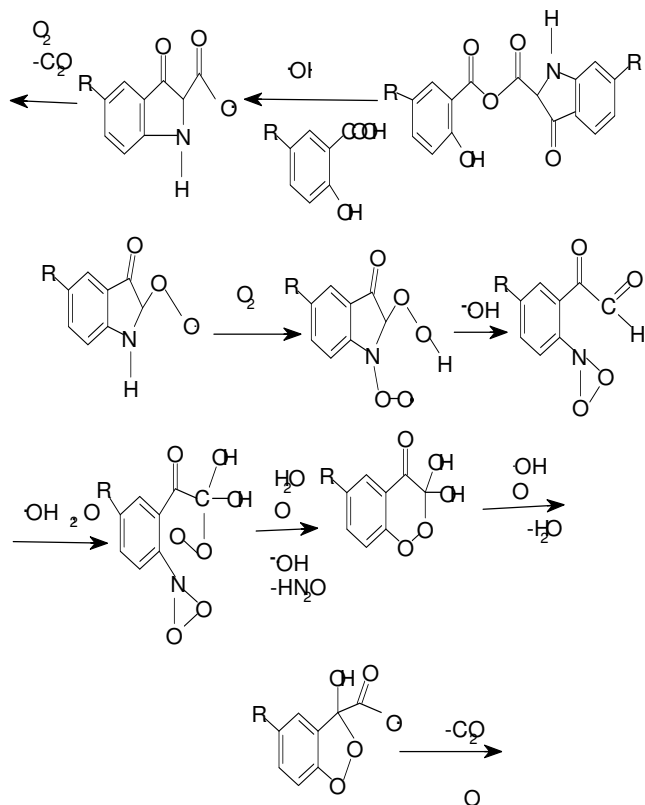
Prof. Badr A. El-sayed, Department of Chemistry, Faculty of Science, Al-Azhar University, Nasr City, Cairo, Egypt.

Dr. Ibrahim A. Ibrahim, Department of Chemistry, Faculty of Science, Al-Azhar University, Nasr City, Cairo, Egypt.

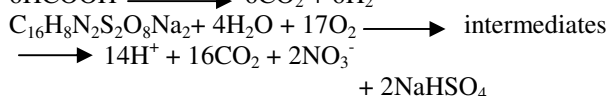
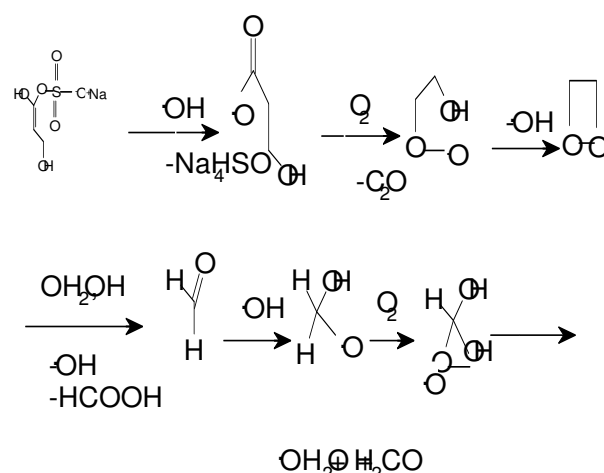
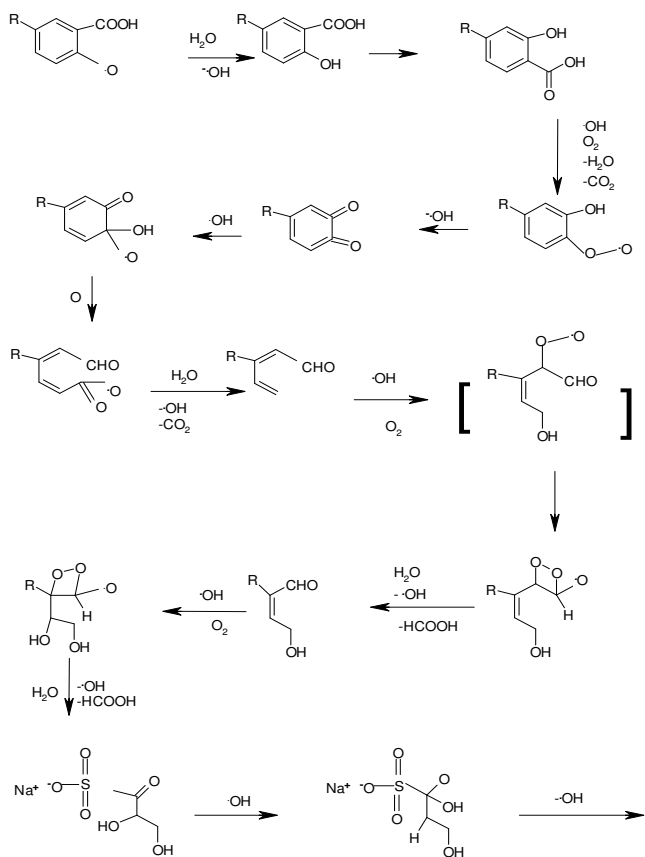
Dr. Walied A. A. Mohamed, Department of Inorganic Chemistry, National Research Center, Giza, Egypt.

Mahmoud A. M. Ahmed, Department of Chemistry, Faculty of Science, Al-Azhar University, Nasr City, Cairo, Egypt.

Synthesis and Characterization of Crystalline Nano TiO₂ and ZnO and their Effects on the Photodegradation of Indigo Carmine Dye



where R = NaSO₃ -



Scheme 1: Probable reaction mechanism for the photocatalytic degradation

Scheme 2 shows the Operation band of a photochemical excited TiO₂ particle. Due to their electronic structure, which is characterized by a filled valence band (VB) and an empty conduction band (CB), semiconductors {metal oxides or sulphides as ZnO, CdS, TiO₂, Fe₂O₃, and ZnS} can act as sensitizers for light induced redox processes. The energy difference between the lowest energy level of the (CB) and the highest energy level of the (VB) is the so-called band gap energy (E_g). It corresponds to the minimum energy of light required to make the material electrically conductive¹⁰.

Scheme 2: Operation of a photochemical excited TiO₂ particle.

When a photon with energy of $h\nu$ exceeds the energy of the band gap, an electron (e^-) is promoted from the (VB) to the (CB) leaving a hole, h^+ , behind. In electrically conducting materials, the produced charge-carriers are immediately recombined. In semiconductors, a portion of this photoexcited electron-hole pairs diffuse to the surface of the catalytic particle (electron-hole pairs are trapped at the surface) and take part in the chemical reaction with the adsorbed donor (D) or acceptor (A) molecules. The holes can oxidize donor molecule as in [1], whereas the

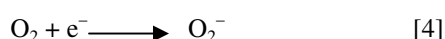
conduction band electrons can reduce appropriate electron acceptor molecules as in [2],



A characteristic feature of semiconducting metal oxides is the strong oxidation power of their holes h^+ . They can react in an one-electron oxidation step with water as in [3], to produce the highly reactive hydroxyl radicals are very powerful oxidant, which can be used to oxidize most organic contaminates.



In general, air oxygen acts as electron acceptor as in “(4),” by forming the super-oxide ion O_2^-

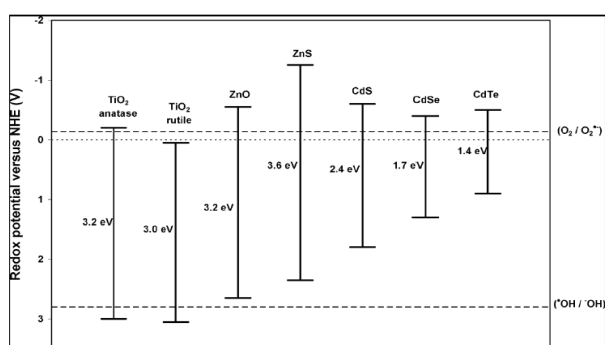


Super – oxide ions are also highly reactive particles, which are able to oxidize materials. The ability of a semiconductor to undergo photoinduced electron transfer to adsorbed particles is governed by the band energy positions of the semiconductor and the redox potentials of the adsorbates, the relevant potential level of the acceptor species is thermodynamically required to be below the conduction band of the semiconductor¹¹.

Table 1: Forbidden energy band gap values for common semiconductors¹².

Semiconductor	E_g (ev)
TiO ₂ (rutile)	3.0
TiO ₂ (anatase)	3.2
ZnO	3.2

Otherwise, the potential level of the donor is required to be above the valence band position of the semiconductor in order to donate an electron to the empty hole. The valence-band holes are power oxidants (+1.0 to +3.5 V Vs NHE depending on the semiconductor and pH), While the conduction-band electrons are good reductants (+0.5 to -1.5 Vs NHE). The band-edge positions of several semiconductors are presented in (Scheme 3).



Scheme 3: Schematics showing energy band gaps and redox potentials for common semiconductors¹³.

This research aims to study the photocatalytic degradation of indigo carmine dye over semiconductive, TiO₂ (28 nm) and ZnO (34 nm) as a photocatalysts. This pigment has been used for many years in industries, such as textile, paper, and plastics, as colorant. Even in very small quantity dyes can be easily recognized either in industrial products or in the wastewaters¹⁴⁻¹⁶. Stability, important property of dyes, prevents treatment of their aqueous residues, even when it is present in low concentrations. Commonly used methods are either economically unfavourable and/or technically complicated¹⁷The effects of doping TiO₂ (28 nm) and ZnO (34 nm) on polyethylene sheet as well as the effects of operational parameters, such as catalyst dose, dye concentration and pH of the solution on the degradation rate of aqueous dye solutions were examined having established optimal operating conditions.

II. MATERIALS AND EXPERIMENTALS

Materials

- Indigo Carmine dye (C₁₆H₈N₂Na₂O₈S₂, M.Wt = 466.36 g/mol, colour index: 73015 purchased from Fluka.
- Tetrabutyl titanate (from Fluka) , trimethyl amine, urea (Alfa Aeser) , ethanol , acetic acid , nitric acid (from Sigma Aldrich) were of analytical reagent grade.
- Zinc 2ethyl hexanoate containing ethylene glycol monomethyl ether supplied by Alfa Aeser.
- TMAH (a tetramethylammonium hydroxide (CH₃)₄NOH), analytical grade was also supplied by Alfa Aeser .
- Water free 2propanol and absolute ethanol supplied by Kemika Ltd (UAE).

II (A). Preparation of TiO₂ Nanoparticles

Firstly, precursor tetrabutyl titanate (20 ml), 10 ml ethanol and 5.0 ml acetic acid were put into a 200 ml flask with stirring for 30 min. to form solution A. 5.0 ml trimethylamine, 6.0 ml distilled water, 2.0 ml nitric acid and 85.0 ml ethanol were mixed with stirring for 10 min. to form solution B. Secondly, solution B was added dropwise into solution A under vigorous stirring until the completion of addition, then slow stirring continued until the solution forms transparent immobile gel. The gel was dried in air flow at 120 °C for 5 hours. The obtained xerogel (Ti (OH)₄) was mixed with urea and ground (the weight ratio of urea to xerogel was 3:1). Finally, the mixture was placed into a Teflon tube that was then placed in a 100 cm³ stainless steel autoclave containing a little water. The autoclave was heated in an oven and kept at 220 °C for 8 hours. The yellow sample powder was obtained after being dried at 110 °C for 1 hour and calcined at 350 °C for 8 hours to obtain pure TiO₂ Nanoparticles after removing any possible precursor residues and urea contaminants.

II (B). Preparation of ZnO Nanoparticles

To 0.982 weight of zinc 2-ethyl hexanoate, 90 ml of 2-propanol was added. After strong mixing a clear (transparent) solution was obtained. Then, 10 ml of (Tetramethylammonium hydroxide) TMAH was added to mixed solution under strong stirring. The formed colloidal suspensions (S1-S4) were aged for 30 min. Washing of the precipitates was performed using a Sorvall RC2-B ultra speed centrifuge (maximum operational range, 20000 rpm)

Synthesis and Characterization of Crystalline Nano TiO₂ and ZnO and their Effects on the Photodegradation of Indigo Carmine Dye

three times with ethanol and two times with distilled water, then dried at 60 °C for 1 hour .

II (C). Preparation of polymer sheets containing nano TiO₂, nano ZnO

TiO₂ Nanoparticle sheets

To 1gm of polyethylene polymer in Petri dish, 0.02 gm of TiO₂ Nanoparticle was added, the mixture was melt by heating to form homogenous thin film of 0.02 gm of TiO₂ Nanoparticle bound polymer. The mixture was then left to dry, the resulting thin film was semitransparent. The method was repeated for 0.04 gm, 0.06 gm, 0.08 gm and 0. 1 gm of TiO₂ Nanoparticle to give different sheets of the TiO₂ Nanoparticle bound polymer.

ZnO Nanoparticle sheets

To 1gm of polyethylene polymer in Petri dish, 0.02 gm of ZnO Nanoparticle was added, the mixture was melt by heating to form homogenous thin film of 0.02 gm of ZnO Nanoparticle bound polymer. The mixture was then left to dry, the resulting thin film was semitransparent. The method was repeated for 0.04 gm, 0.06 gm, 0.08 gm and 0.1 gm of ZnO Nanoparticle to give different sheets of the ZnO Nanoparticle bound polymer.

Scanning electron microscope (SEM)

The scanning electron micrographs were recorded with Philips XL-30 SEM analyzer (JEOL – JSM – T 330 A) with an acceleration voltage 30 KV for characterization the surface morphology of TiO₂ and ZnO photocatalysts.

The X-ray diffraction (XRD)

The X-ray diffraction of TiO₂ (28 nm) and ZnO (34 nm) powders were recorded by Philips Holland. Xpert MPD model using Cu-Kα target.

III. RESULTS AND DISCUSSION

III (A). Characterization of highly Crystalline Nano TiO₂ and ZnO :

SEM Analysis

The SEM photographs (Figure 1-4) depict the surface texture and porosity, before and after treatment of photocatalysts.

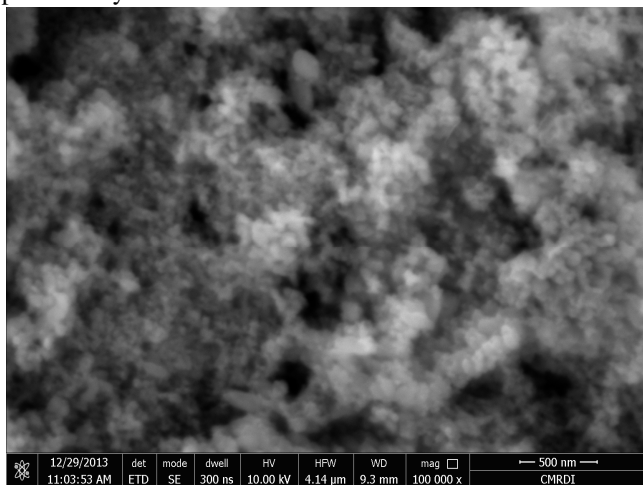


Figure 1: Scanning electron microscope (SEM) of TiO₂ (anatase) at (X 100000).

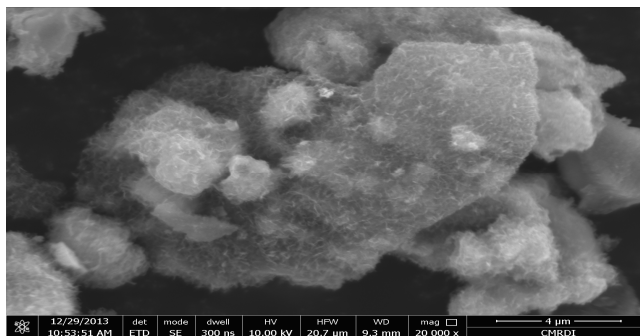


Figure 2: Scanning electron microscope (SEM) of TiO₂ (28 nm) at (X 20000).

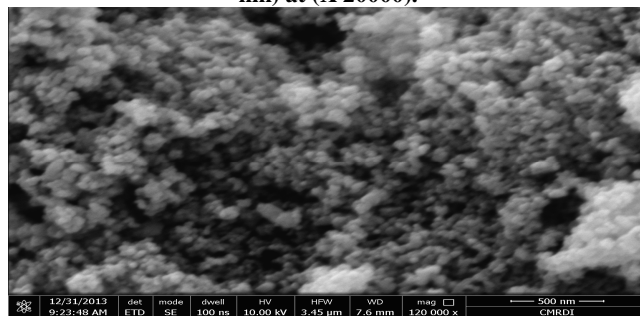


Figure 3: Scanning electron microscope (SEM) of ZnO at (X 120000).

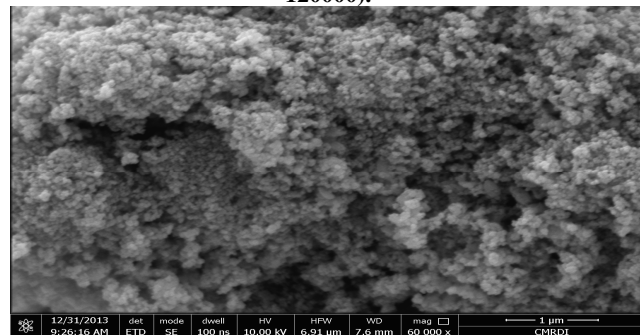


Figure 4: Scanning electron microscope (SEM) of ZnO (34 nm) at (X 60000).

XRD Analysis

It is well known that the X-ray diffraction patterns of TiO₂ and ZnO were observed at 25.25° and 31.78° respectively¹⁸. The X-ray diffraction patterns show a shift to 26.64° for TiO₂ (28 nm) and a shift to 37.76° for ZnO (34 nm) indicating the interrelation of surfactant ions in the ZnO as shown in (Figure 5 and 6) respectively. On the other hand the d values for TiO₂ and ZnO observed at 0.5764 and 0.4706 respectively¹⁸ were observed at 0.4583 and 0.4012 respectively as shown in (Figure 5 and 6)

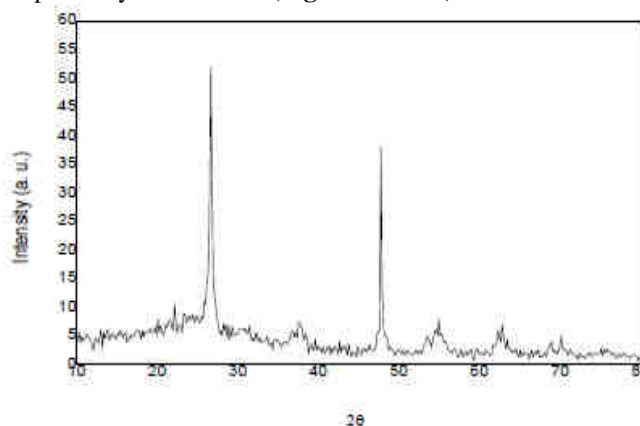


Figure 5: XRD diagram of nano TiO₂

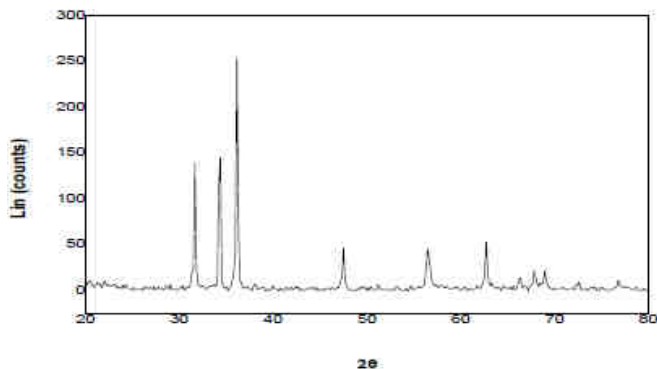


Figure 6: XRD diagram of nano ZnO

III (B). Effect of the initial dye concentration

The effects of the initial concentration of Indigo Carmine (IC) dye on the photocatalytic efficiency was investigated with concentrations 1.0×10^{-5} M, 1.5×10^{-5} M, 2.0×10^{-5} M, 2.5×10^{-5} M, and 3.0×10^{-5} M (Figure 7). Generally it was found that on increasing the dye concentration the degradation efficiencies of dye decreases. Hence, the photo-oxidation process will work faster at a low concentration of pollutants. These results are in agreement with previous reports¹⁹⁻²¹ that photodegradation of textile dye Reactive Red 2, C.I. Acid Yellow 17, and Direct Yellow12 decreased with increasing concentrations. At high concentrations of dye, the deeper coloured solution would be less transparent to UV light and the dye molecules may absorb a significant amount of UV light causing less light to reach the catalyst and thus reducing the OH[•] radical formation. Since OH[•] radicals are of prime importance in the attack of the dye molecules, lowering the amount OH[•] radicals would cause the photodegradation efficiency to decrease.

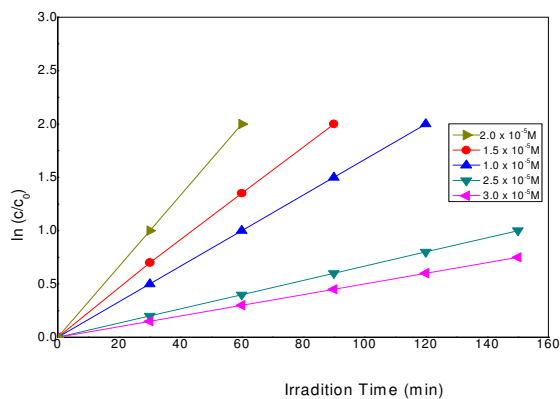


Figure 7: Effect of indigo carmine concentration during photodegradation process.

III (C). Effect of photocatalyst dopent

The photocatalyst dopent was studied with varying photocatalysis as Nano TiO₂ and ZnO dopent with 0.02 g/l to 0.1 g/l at pH 6.3 (Figure 8-11). the percentage of removal of the dyes increases with increasing in quantity of the photocatalyst. The activity of the photocatalyst increased with a decreasing the nano-sized TiO₂ and ZnO. However, the % removal rate of the dye is as faster at the smaller nano-sized TiO₂ or ZnO with an increase in the concentration of nanophotocatalyst.

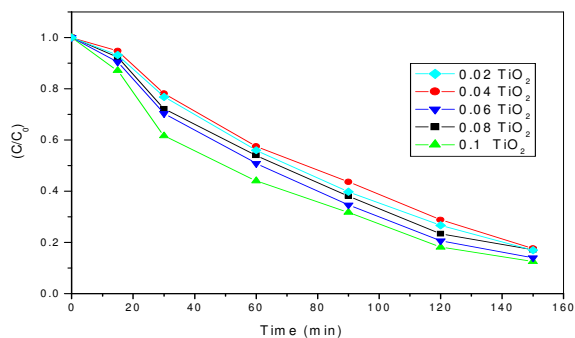


Figure 8: Effect of TiO2 (commercial) concentration.

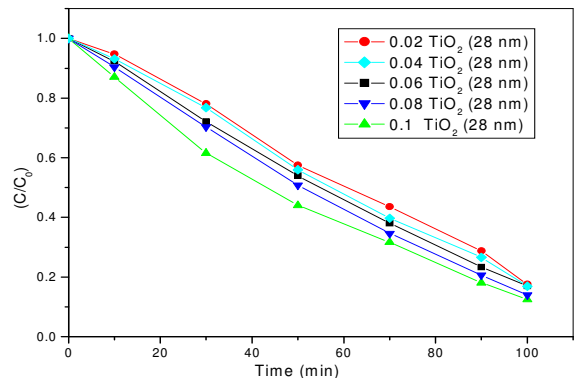


Figure 9: Effect of TiO2 (28 nm) concentration.

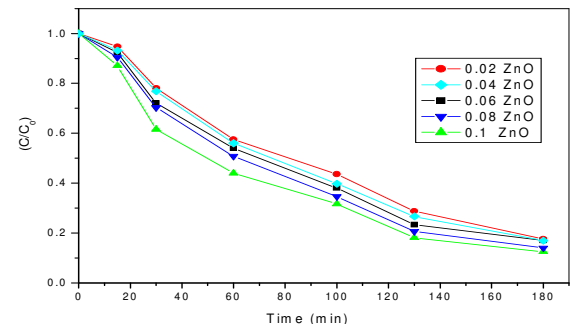


Figure 10: Effect of ZnO (commercial) concentration.

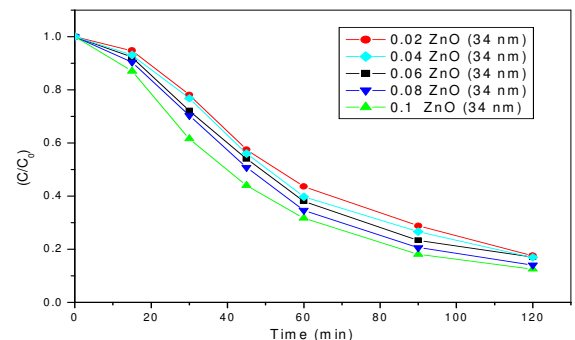


Figure 11: Effect of ZnO (34 nm) concentration.

III (D). Photocatalytic degradation of indigo carmine (IC)

The photodegradation efficiencies of IC in the presence of different nanoxides (Titanium dioxideTiO₂ and Zinc oxide ZnO) under UV light irradiation were shown in (Figure 9-11). The cracked surface of TiO₂ has grooves running all over the surface. These grooves give the sheet at least two advantages: (i) after falling into the groove, the dye

Synthesis and Characterization of Crystalline Nano TiO₂ and ZnO and their Effects on the Photodegradation of Indigo Carmine Dye

molecules can not easily escape from the surface, and (ii) along the groove surface, the oxygen atoms have a better chance to protrude from the latex texture and their negative charges can attract or repel charges of the dye molecular fragment. It is well known that the smoother surface of ZnO with TiO₂ particles embedded deeper in the surface will have weaker electrostatic forces to interact with the dye molecules. Therefore, the higher surface roughness can help to gather more dye molecules onto the surface and more photocatalytic reaction can take place. This is reflected by the slightly better performance of TiO₂ over ZnO as shown in (Figure 8-11). The kinetics of photodegradation were studied and the data were tested with the first-order kinetic expression [5],²¹⁻²²

$$\ln[C_t] = \ln[C_0] - k_{app}t \quad [5]$$

where [C₀] is the initial concentration of dye, [C_t] is the concentration at time t, and k_{app} is the apparent rate constant. The straight lines obtained when ln[C_t] was plotted against t confirmed the first-order kinetics of dye degradation. The rate constants for IC dye degradation were found to be 0.717 ± 0.004 h⁻¹ and 0.595 ± 0.004 h⁻¹ for the TiO₂ and ZnO, respectively (n = 3).

Adsorption tests in dark were carried out in order to evaluate the equilibrium constants of adsorbed dye on the photocatalyst surface.

The high UV light intensity increases the photon in flux entering the dye solution and consequently excites the TiO₂ particles and more OH[•] radicals being formed at the surface. As the reactive number of OH[•] radicals attacking the dye molecules increases, the photodegradation efficiency also increases. The activity increases with irradiation time up to 210 min. of UV light, while it is nearly stable in dark reaction up to 60 min. as in (Figure 12).

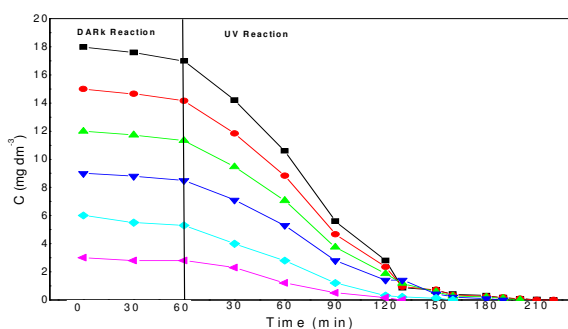


Figure 12: Effect of IC concentrations adsorbed on the surface in two segments (Dark and UV)

III (E). Effect of pH

All of the experiments were carried out at the natural pH of IC dye water solution which is 6.3. However, in real life situations the effluents from factories may cover a wide range of pHs. To assess the efficiencies of photodegradation by the TiO₂ (28 nm), solutions of several pH values (3, 5, 8 and 12) were investigated. Both TiO₂ (28 nm) and ZnO (34 nm) showed parallel behaviour (Figure 13-14). Generally, for a charged surface containing TiO₂ particles, a significant dependence of the photocatalytic efficiency on the pH value is observed, since the overall surface charge and hence the

adsorptive properties of TiO₂ particles depend strongly on the solution pH. It is known that the metal oxide particles in water exhibit amphoteric behaviour and readily react with dye by a mechanism which can be described by the following chemical equilibria^{7, 23 and 24}.



The charge of TiO₂ depends on the solution pH. The pH at the point of zero charge (pH_{PZC}) for TiO₂ has been reported to be in the range 6.25–6.75²⁵. Thus, the TiO₂ surface is positively charged in acidic media (pH < pH_{PZC}), and negatively charged under alkaline conditions (pH > pH_{PZC}). This argument valid for the powder form in contact with solution, Therefore, it is expected that at a pH below pH_{PZC}, the TiO₂ surface acquires a positive charge, indicated by [6] and hence attracts the negatively charged IC dye skeleton resulting in a large number of dye molecules being attracted (or adsorbed) onto the TiO₂ doped in the surface of polymer sheet. At a pH above pH_{PZC}, electrostatic repulsion between the negative charge at the TiO₂ surface, as shown in [7] and anionic dye skeleton retards the accumulation of dye molecules at the surface resulting in decrease of the photodegradation activity. Attacking the dye molecules increases, the photodegradation efficiency also increases.

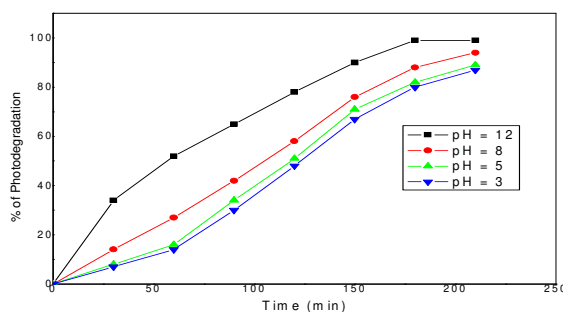


Figure 13: Effect of pH on the photodegradation efficiency of IC dye by TiO₂ (28 nm).

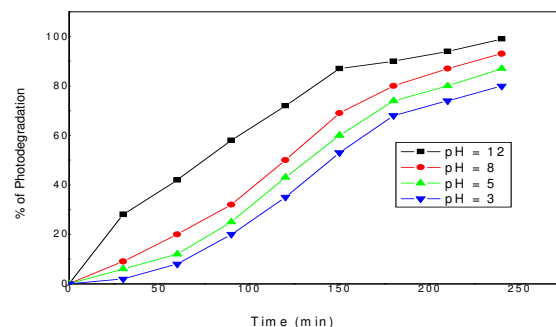


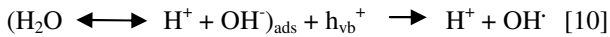
Figure 14: Effect of pH on the photodegradation efficiency of IC dye by ZnO (34 nm).

III (F). Reaction mechanism for the photocatalytic degradation of Organic dyes

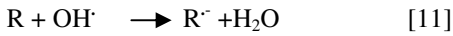
A mechanism of the photocatalytic degradation of organic dyes can be described by following steps²⁶. Absorption of photons by TiO₂ and production of photoholes and electron pairs



Neutralization of OH⁻ by photoholes



Reaction of an organic dye with OH⁻ radical or directly with the holes



The completely suggested mechanism for the photochemical degradation of the organic dye was suggested⁸.

III (G). Determination of pKa values

The ratio of the molecular and ionic forms of an acid or base at a given pH can be calculated from the pK_a value using [14],

$$K_a = \frac{[H^+][D]}{[P]} \quad [13]$$

$$pK_a = pH + \log \frac{[D]}{[P]} \quad [14]$$

Where K_a is the dissolution constant of the acidic or the protonated base, [D] and [P] are the concentrations of the deprotonated and protonated forms possessing separate spectra. With the exception of those cases where the aim of the absorbance measurement is to study protolytic equilibrium (especially in the case of quantitative analysis), measurements are carried out at different pH values, which assure the presence of either the fully protonated or fully deprotonated forms. Equation [13] is not only suitable for the calculation of the expected pH range protonation-deprotonation, but it can be used for determination of the dissociation constants at the pH causing considerable changes in their spectra, [14] is used. A more accurate calculation method is used to compute the pK_a value at all pH values separately when two forms, ionic and molecular, are present in commensurable concentrations. When the functional group is being determined as an acid, A_D is greater than A_P, [15] and [16] are used, and if the reverse occurs [17] and [18] are used.

$$pK_a = pH + \log \frac{[P]}{[D]} = pH + \log \frac{A_D - A}{A - A_P} \quad [15]$$

Then,

$$pH = pK_a - \log \frac{[P]}{[D]} = pK_a - \log \frac{A_D - A}{A - A_P} \quad [16]$$

The values of $\log \frac{A_D - A}{A - A_P}$ can be plotted against the different pH values to give a straight line with intercept equal to the pK_a value.

$$pK_a = pH + \log \frac{[P]}{[D]} = pH + \log \frac{A - A_D}{A_P - A} \quad [17]$$

Then

$$pH = pK_a - \log \frac{[P]}{[D]} = pK_a - \log \frac{A - A_D}{A_P - A} \quad [18]$$

When the functional group is determined as a base [19] and [20] are used when A_D is greater than A_P, and if the reverse occurs [21] and [22] are used.

$$pK_a = pH + \log \frac{[P]}{[D]} = pH + \log \frac{A - A_P}{A_D - A} \quad [19]$$

Then

$$pH = pK_a - \log \frac{[P]}{[D]} = pK_a - \log \frac{A - A_P}{A_D - A} \quad [20]$$

Similarly, the values of $\log \frac{A - A_P}{A_D - A}$ can be plotted against the different pH values to give a straight line with intercept equal to the pK_a value²⁷.

$$pK_a = pH + \log \frac{[P]}{[D]} = pH + \log \frac{A_P - A}{A - A_D} \quad [21]$$

Then

$$pH = pK_a - \log \frac{[P]}{[D]} = pK_a - \log \frac{A_P - A}{A - A_D} \quad [22]$$

Indigo Carmine absorbs strongly in the visible region and shows absorption intensity bands around 475 nm in acidic media indicating the charge migration over the whole molecule (charge transfer-transition). In basic media these bands are shifted to longer wavelength at around 606 nm that is to be due to extensive charge dispersion in the basic form of Indigo Carmine. The pK_a can be determined by the following two methods:

Method (I)

Determination of pK_a is represented in (Figure 15) by using data of the absorption value for the two peaks at 475 and 606 nm. The pK_a was determined at the intersection point²⁸ (pH = 12.99).

Table 2: Absorption spectral data of Indigo Carmine in different pH Media.

pH	Absorbance values	
	At 475 nm	At 606 nm
2.8	0.187	2.198
3	0.154	2.122
4	0.151	2.024
5	0.142	2.00
6	0.177	1.93
7	0.197	1.92
8	0.085	1.10
9	0.072	1.01
10	0.047	0.58
11	0.037	0.24
12	0.018	0.18
13	0.122	0.10
13.3	0.02	0.069

Synthesis and Characterization of Crystalline Nano TiO₂ and ZnO and their Effects on the Photodegradation of Indigo Carmine Dye

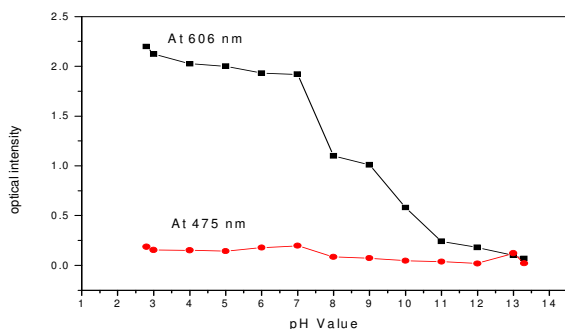


Figure 15: Determination of pKa value of Indigo Carmine in different pH media.

Method (II)

pKa value also could be determined mathematically using the absorption spectral data showed in (Table 3) by applying the following equation [23]²⁹.

$$pKa = pH + \log \frac{AD-A}{A-AP} \quad [23]$$

Where AD and AP are the observed optical densities (absorbance values) of the fully deprotonated and protonated forms, respectively. A is the absorbance values of basic peaks at 606 nm at different pH values. Where A_D (value of the fully deprotonated form) = 2.198, A_P (value of the fully protonated form) = 0.02 and A is the absorbance values of basic peaks at 606 nm at different pH values, the calculated pKa is 11.17

Table 3: Determination of pKa of Indigo Carmine in different pH Media.

pH	AD-A	A-AP	$\log \frac{AD-A}{A-AP}$	$pKa = pH + \log \frac{AD-A}{A-AP}$
8	1.098	1.08	0.00717	8.00717
9	1.188	0.99	0.07918	9.07918
10	1.618	0.56	0.46079	10.4607
11	1.958	0.22	0.94939	11.9493
12	2.018	0.16	1.10080	13.1008
13	2.098	0.08	1.41871	14.4187

IV. CONCLUSION

The photocatalytic degradation was obviously affected by the initial concentration with respect to Langmuir-Hinshelwood kinetic model. photodegradation of Indigo Carmine dye was successfully carried out using both TiO₂ (28 nm) and ZnO (34 nm). In the present study, the efficiency of photocatalytic degradation of indigo carmine dye solution using TiO₂ (28 nm) and ZnO (34 nm) in presence of UV light has been studied, the effect of catalyst loading, initial concentration of the dye, effect of pH and pKa value have been reported. The experimental results demonstrated that the optimal catalyst concentration of TiO₂ (28 nm) and ZnO (34 nm) was 0.1 g with indigo carmine concentration of 2×10⁻⁵ M. The optimal operation pH was 12 and the pKa value of the dye was 12.99 in method (I) and 11.17 in method (II).

REFERENCES

1. M. Double., A. Kumar, Biotreatment of Industrial Effluents. Elsevier, Amsterdam, The Netherlands Eunyoung B., Wonyong C., 2003, Highly Enhanced Photoreductive Degradation of Perchlorinated

2. Compounds on Dye-Sensitized Metal/TiO₂ under Visible Light, Environmental Science & Technology, (2005), 37, 147-152.
3. G. Sachin. Ghugal, S. Suresh. Umare and Rajamma Sasikala, RSC Adv., (2015) 5, 63393
4. British Journal of Environmental Sciences, (December 2014), Vol.2, No.4, pp.29-40.
5. International Journal of Chemical Sciences and Applications, (2014), Vol. 5, Issue 1, pp 1-6.
6. I. T. Peternel, N. Koprivanac, A.M. Locaric Bozic, H.M. Kusic, Comparative study of a UV/TiO₂, UV/ZnO and photo-Fenton processes for the organic reactive dye degradation in aqueous solution, Journal of Hazardous Material, 2007, 148, 477-484.
7. Haarstrick, O.M. Kut, E. Heinze, TiO₂-Assisted Degradation of Environmentally Relevant Organic Compounds in wastewater Using a Novel Fluidized Bed Photoreactor, Environmental Science & Technology, 1996, 30, 817-824.
8. H. Lachheb, E. Puzenat, A. Houas, M. Ksibi, E. Elaloui, C. Guillard, J. M. Herrmann., Photocatalytic degradation of various types of dyes (Alizarin S, Crocein Orange G, Methyl red, Congo Red, Methylene blue) in water by UV- irradiated titania, Applied Catalysis B: Environmental, 2002, 39, 75-90.
9. B V Suresh Kumar, C P Sajan, K M Lokanatha Rai, K Byrappa, Indian Journal of chemical technology May 2010, Vol. 17, pp. 191-197.
10. M. Vořnov and J. Augustynski., (1997). "Heterogeneous Photocatalysis", Vol., John wiley & sons LTD, Bafins Lane, Chichester, West Sussex PO19 1UD, England.
11. Hagfeldt Anders, Michel Gratzel, (1995) "light induced redox reactions in nanocrystalline systems", Chem Rev, 95, 49- 68.
12. Sobczykński, A. Dobosz, Water Purification by Photocatalysis on Semiconductors, Polish Journal of Environmental Studies, . 2001, 10, 195.
13. A. L. Linseigler, G. Lu, T. John Yates, (1995), Photocatalysis on TiO₂ Surfaces: Principles, Mechanisms, and Selected Results, Chem. Rev, 95, 735.
14. R. Benedix, F. Dehan and J. Quaas, (2000), Application of Titanium Dioxide Photocatalysis to Create Self-cleaning Building Materials, LACER, Vol.5.
15. T. Robinson, G. McMullan, R. Marchant, P. Nigam, Bioresour. Technol., 2001, 77, 247.
16. I. M. Banat, P. Nigam, D. Singh, R. Marchant, Microbial decolorization of textile-dye-containing effluents: a review. Bioresour Technol, 1996, 58, 217-227.
17. Z. Zainal, L.K. Hui, M. Z. Hussein, Y.H. Taufiq-Yap, A. H. Abdullah, I. Ramli, Removal of dyes using immobilized titanium dioxide illuminated by fluorescent lamps. J. Haz. Mat., 2005, 125, 113-120.
18. C. Hachem, F. Bocquillon, O. Zahraa, M. Bouchy, Decolourization of textile industry wastewater by the photocatalytic degradation process., Dyes and Pigments, 2001, 49, 117-125.
19. K. M. Joshi et al Arch. Appl. Sci Res., 2011, 3(2):596-605.
20. CC Liu, YH Hsieh, PF Lai, CH Li, CL Kao, Photodegradation treatment of azo dye wastewater by UV/TiO₂ process., Dyes Pigments, 2006, 68, 5-191.
21. F Kiriakidou, DI Kondarides, XE Verykios, The effect of operational parameters and TiO₂ doping on the photocatalytic degradation of azo-dyes., Catalysis Today, 1999, 54, 30-119.
22. S Senthilkumaar, K Porkodi, Heterogeneous photocatalytic decomposition of Crystal Violet in UV illuminated sol-gel derived nanocrystalline TiO₂ suspension., J. of Colloid Interface Sci., 2005, 288, 9-184.
23. CG Silva, W. Wong, JL Faria., Photocatalytic and photochemical degradation of mono-di-and triazo dye in aqueous solution by UV irradiation., J. of Photochem. Photobiol. A, 2006, 181, 24-314.
24. Langmuir, J. Am. Chem. Soc., 1918, 40 1361-1403.
25. AP Toor, A Verma, CK Jotshi, PK Bajpai, V Singh., Photocatalytic degradation of Direct Yellow 12 dye using UV/TiO₂ in a shallow pound slurry reactor., Dyes Pigments, 2006, 68, 53-60.
26. J Sun, L Qiao, S Sun, G Wang, Photocatalytic degradation of Orange G on nitrogen- doped TiO₂ catalyst under visible light and sunlight irradiation, J. Hazard Mater, 2008, 155, 9-312.
27. M. Vautier, C. Guillard, J.-M. Herrmann, Photocatalytic Degradation of Dyes in Water: Case Study of Indigo and of Indigo Carmine, Journal of Catalysis, 2001, 201, 46-59.
28. S. Görög , Ultraviolet-Visible Spectroscopy in Pharmaceutical Analysis CRS Press (Boca Raton New York London Tokyo) Inc. (1995); 82-90 .
29. R.I. Allen, K.J. Box, J.E.A. Comer, C. Peake, K.Y. Tam, J. Pharm. Biomed. Anal., 1998, 17 699.
30. P. Maroni and J. P. Calmon, Bull. Soc. Chim. Fr., 1964, 519.